Sustainable Materials and Technologies 3 (2015) 17–28

Contents lists available at ScienceDirect

Sustainable Materials and Technologies

Optimization of enzymatic saccharification of water hyacinth biomass for bio-ethanol: Comparison between artificial neural network and response surface methodology

S. Das [a], A. Bhattacharya [b], S. Haldar [b], A. Ganguly [c], Sai Gu [d], Y.P. Ting [a], P.K. Chatterjee [c,*]

[a] Department of Chemical and Biomolecular Engineering, National University of Singapore, Singapore
[b] Nation Institute of Technology, Durgapur 713209, India
[c] Thermal Engineering Division Central Mechanical Engineering Research Institute, Durgapur 713209, India
[d] Centre for Renewable Energy and Biofuels, Cranfield University, UK

ARTICLE INFO

Article history:
Received 25 November 2014
Received in revised form 30 January 2015
Accepted 30 January 2015
Available online 11 February 2015

Keywords:
Response surface methodology
Artificial neural network
Genetic algorithm
Enzymatic saccharification
Water hyacinth biomass
Bio-ethanol

ABSTRACT

Response surface methodology (RSM) is commonly used for optimising process parameters affecting enzymatic hydrolysis. However, artificial neural network–genetic algorithm hybrid model can also serve as an effective option, primarily for non-linear polynomial systems. The present study compares these approaches for enzymatic hydrolysis of water hyacinth biomass to maximise total reducing sugar (TRS) for bio-ethanol production. Maximum TRS (0.5672 g/g) was obtained using 9.92 (% w/w) substrate concentrations, 49.56 U/g cellulase concentrations, 280.33 U/g xylanase concentrations and 0.13 (% w/w) surfactant concentrations. The average % error for artificial neural networking (ANN) and RSM were 3.08 and 4.82 and the prediction percentage errors in optimum output are 0.95 and 1.41, respectively, which showed the supremacy of ANN in illustrating the non-linear behaviour of the system. Fermentation of the hydrolysate yielded a maximum ethanol concentration of 10.44 g/l using *Pichia stipitis*, followed by 8.24 and 6.76 g/l for *Candida shehatae* and *Saccharomyces cerevisiae*.

1. Introduction

Recently, a substantial hike in the fossil fuel prices due to the rapid depletion of natural energy sources and human population explosion has kindled immense public cognizance towards global energy security [1]. Factors like global warming, environmental considerations and sustainable growth are encouraging scientists to explore low cost, environment friendly alternative energy sources [2]. In a forage for sustainable replacement of fossil fuels, lignocellulosic biomass derived biofuel can be an alternative renewable energy. Their major advantages are abundant availability, sustainability, recyclability, carbon neutrality and absence of 'food vs. fuel' competition [3]. The residual biomass can also be converted into other value added platform chemicals in a well-integrated biorefinery facility. According to Demirbas [4], integrated biorefinery is an establishment where biomass is converted into fuels, power and value added chemicals with minimum waste generation.

Water hyacinth *(Eichhornia crassipes)* is widely found in tropical countries, like India. It is a noxious weed which rapidly depletes the nutrient and oxygen content of the water, thereby affecting the flora and fauna of the ecosystem. Under favourable conditions, water hyacinth can achieve a growth rate of 17.5 metric tonnes per hectare per day [5]. Large availability of water hyacinth makes it an attractive raw material. Conversion of waste water hyacinth biomass (WHB) to biogas and bio-ethanol has already been explored [6,7].

Conversion of biomass to bio-ethanol mainly comprises of following steps: pre-treatment, saccharification and fermentation. Naïve lignocellulosic biomass is generally recalcitrant to microbial and mechanical degradation, thus rendering it difficult to extract fermentable sugars. Lignin, one of the major components of lignocellulosic biomass, is impediment to enzymatic saccharification [8]. Hence, de-lignification can substantially improve the enzymatic saccharification of the biomass. It has been observed that pre-treatment of WHB with sodium hydroxide is an effective delignification strategy [2].

The major factors that affect the efficiency of the enzymatic saccharification of WHB are substrate concentration, enzyme loading, incubation time and surfactant concentration. The current study has two main objectives, viz. (i) maximizing yield of reducing sugars by enzymatic saccharification to enhance bioethanol production and (ii) comparing the performance of statistical and artificial intelligence-based techniques while optimising process parameters of the enzymatic saccharification of WHB. Traditional 'single-factor-at-a-time' optimisation technique is arduous, time taking and may not assure optimum condition. Hence, Artificial neural network-Genetic algorithm (ANN-GA) and Response surface methodology (RSM) have been implemented to study these interaction effects of the process parameters: substrate

* Corresponding author.
E-mail address: pradipcmeri@gmail.com (P.K. Chatterjee).

http://dx.doi.org/10.1016/j.susmat.2015.01.001

concentration, enzyme loading and surfactant concentration for maximum yield of reducing sugar during enzymatic saccharification. The optimal condition is verified experimentally and compared to determine the efficiency of both RSM and ANN-GA hybrid technique, which may be the first study on comparison of ANN-GA and RSM for enzymatic hydrolysis of water hyacinth using cellulase and xylanase enzymes to maximise reducing sugar yield for bioethanol production.

2. Materials and methods

2.1. Biomass feedstock

Water hyacinth (*Eichhornia crassipes*) plants were obtained from a pond within the premises of Central Mechanical Engineering Research Institute, Durgapur, India. The shoots and the leaves were initially reduced to a particle size of 2–3 cm and then dried at 106 °C for 6 hours. After drying, the particle size of the biomass was further reduced to 1 mm in a knife mill and stored in air tight containers.

2.2. Alkali pre-treatment of water hyacinth biomass

WHB was delignified by pre-treating the biomass by sodium hydroxide in 250 ml Erlenmeyer flasks with a biomass loading of 10% (w/v), 5% (w/v) concentration of sodium hydroxide, soaking time of 1 hour and treatment time of 10 minutes at 130 °C. The pre-treated sample was neutralised and washed repeatedly and then dried.

2.3. Feedstock compositional analysis

National Renewable Energy Laboratory (NREL) analytical protocol was followed to evaluate the composition of WHB [9]. 72 % (v/v) sulphuric acid was added to 300 mg of biomass and was treated for 1 hour at 30 °C. The acid concentration was diluted to 4% (v/v) with de-ionised water. The diluted mixture was autoclaved at 121 °C for 1 hour. After autoclave the mixture is filtered using 0.2 μm filters for HPLC analysis. The solid residue was used to estimate the acid insoluble lignin.

2.4. Physicochemical characterisation of biomass

Physico-chemical characterisations were performed to examine the changes in the biomass after different stages.

2.4.1. Scanning electron microscopy

Scanning Electron Microscope (SEM) (JEOLJSM-5600) analysis was performed to identify the structural transformation.

2.4.2. X-Ray diffraction analysis

X-Ray Diffraction (XRD) was implemented to determine the crystallinity index (CrI) of the WHB using Shimadzu XRD-6000 diffractometer. The range of the X-Ray Diffractogram is scanned between 10–30° with a step size of 0.0205 using Cu-Kα radiation X-Ray (λ = 1.54 Å) generated at a voltage of 40 kV and 30 mA current. CrI of the sample was calculated as follows [10]:

$$\mathrm{CrI}(\%) = \left[\frac{(I_{002} - I_{14.7^o})}{I_{002}}\right] \times 100 \quad (1)$$

where I_{002} is the maximum intensity at the (002) lattice diffraction at $2\theta = 22.4°$ and $I^{o}_{14.7}$ is the intensity of the background scatter at $2\theta = 14.7°$.

To calculate the crystalline size the following equation was used:

$$D(hkl) = \frac{\lambda\kappa}{\beta_o \cos\theta} \quad (2)$$

where D (hkl) signifies the size of the crystallite (nm), 'κ' is the Scherrer constant (0.94), 'λ' is the X-Ray wavelength (for copper the value of 'λ' is 0.1548 nm), β_o is the full width at half of the maximum height of the reflection at hkl measured at 2θ Bragg's angle.

Degree of crystallinity has been calculated using the following equation [11]:

$$\eta_c = \frac{A_c}{A_a + A_c} \times 100 \quad (3)$$

where η_c is the degree of crystallinity, and A_c and A_a denotes the area of the crystalline and non-crystalline regions respectively.

2.4.3. Fourier transform infrared spectroscopy (FTIR)

FTIR spectroscopy is a powerful analytical technique to examine the functional groups of a polysaccharide. IR spectra were studied using Shimadzu spectrometer (Japan). Samples were prepared by mixing 2 mg of biomass and 198 mg of spectroscopic grade KBr. After grinding, the mixture was pressed to form disks. The spectra were generated with an average scan of 16 scans with a resolution of 4 cm^{-1} within a range of 4000–400 cm^{-1}.

2.4.4. Biomass saccharification

Cellulase from *Trichoderma reesei* and xylanase from *Trametes versicolor* were obtained from Sigma Aldrich®. Enzymatic saccharification of alkali pre-treated WHB were carried out in 50 mM citrate buffer (pH 4.8), at 50 °C in 100 ml stoppered flasks with an agitation speed of 150 rpm for 60 hours. Tween-80 was added as surfactant. The reducing sugars (glucose, xylose, arabinose and mannose) were monitored by 2, 5-dinitrosalicyclic acid method [12]. The hydrolysate was centrifuged at 10,000 rpm for 10 minutes at 4 °C. The supernatant collected was filter sterilised for fermentation experiments.

2.5. Experimental designs and optimisation strategy

2.5.1. Artificial neural network modelling

Artificial neural network (ANN) modelling can be an excellent alternative to Response Surface Methodology (RSM) for solving regression based problems of polynomial non-linear systems. ANN architecture is made of highly interlinked bundles of elements called neurons [13], the connections between the neurons defined by weights (w) and biases (b). The neurons are controlled by a defined transfer and a summing function. The most commonly used transfer functions are: *purelin, log sig and tan sig* [14]. A multi-layer neural architecture consists of input, output and hidden layer. Multi-layer feed-forward neural network also known as multi-layer perceptron (MLP) helps in effective management of the neural architecture while solving non-linear regression models. In this study, the predictive model has been built using substrate concentration (% w/w), xylanase loading (U/g), cellulase loading (U/g) and surfactant concentration (% w/w) as the input parameters, and yield of reducing sugar (mg/g) as the output for the model. The function of the input layer is to present the scaled input data to the hidden layer through weights. The hidden layer then sums up the weighted inputs along with the biases as:

$$\mathrm{sum} = \sum_{i=1}^{n} x_i w_i + \theta \quad (4)$$

where, w_i (i = 1,n) represents the weights of the connection between the neurons of the input and the hidden layer, θ is defined as the bias and x_i signifies the input parameter. An activation function is used to transfer the weighted output to a non-linear domain.

The data set formed after hidden layer operation was considered as the input for the output layer. The final predicted response by the ANN model was generated by the output layer. A mean-squared error function was developed using the predicted response and actual

experimental outcome. Then the weights and biases were adjusted by error-back-propagation (EBP) training algorithm to minimise the error function [15].

2.5.2. Genetic algorithm

After developing the ANN model, genetic algorithm (GA) was used to optimise the input data set. GA uses stochastic search approach for process optimisation. It is an evolutionary algorithm that follows Darwin's theory of 'survival of the fittest' [16]. GA follows four simple steps (Fig. 1). The algorithm at first initializes a random solution set as the initial population, i.e. ($s_1^{(k)}$, $s_2^{(k)}$, $s_3^{(k)}$ ….$s_z^{(k)}$), where 'z' represents the number of individuals and 'k' implies the number of iterations/generations. The individuals in the current population matrix is known as chromosomes ($s_1^{(k)}$). The components of chromosome can be defined as genes. The evaluation of the fitness function can be represented as: ($f(s_1^{(k)})$, $f(s_2^{(k)})$, $f(s_3^{(k)})$, ….. $f(s_z^{(k)})$). A stop criterion is defined which is checked after evaluation. If the stop criterion is satisfied, the optimal condition is achieved and the result is saved and returned. If not, then the current population is sorted and ranked. A selected set of individuals termed as parental chromosomes ($s_1^{(k)}$, $s_2^{(k)}$, $s_3^{(k)}$, ….. $s_{a-s}^{(k)}$) is used to generate a set of off-springs to generate the next generation ($s_1^{(k+1)}$, $s_2^{(k+1)}$, $s_3^{(k+1)}$ ….. $s_z^{(k+1)}$) by performing operations like crossover, mutation and reproduction [17]. After several sets of iterations, the algorithm converges to the optimal solution.

2.5.3. Response surface methodology (RSM)

RSM incorporates mathematical and modelling techniques to build an experimental design for solving multivariate equations [18]. In the present, RSM was used to develop an experimental design to evaluate the optimum condition for maximizing total reducing sugar yield. Box-Behnken model was implemented to investigate the interaction effects. To gauge the variability in the measurements, all the experiments were performed in triplicates. A second order polynomial equation (Eq. (5)) was used to estimate the relationship between the independent and the experimental responses:

$$Y = \beta_o + \sum_{i=1}^{k} \beta_i X_i + \sum_{i}^{k} \beta_{ii} X_i X_i + \sum_{i=1}^{k-1} \sum_{j=i+1}^{k} \beta_{ij} X_i X_j \quad (5)$$

where 'Y' is the predicted response, β_o is constant, β_i represents the linear co-efficient, β_{ii} implies the co-efficient of the squared terms, β_{ij} expresses the co-efficient of the cross term products and 'k' indicates the number of independent factors in the optimisation study.

Design Expert Version 8.0.10 was used to develop the experimental model and estimate the co-efficient of the second-order-polynomial. The range of the independent parameters and the experimental design setup along with responses were defined in Tables 1 and 2 respectively.

2.6. Fermentation

Pichia stipitis (NCIM 3500) and *Candida shehatae* (NCIM 3497) were used in the fermentation as these yeasts are capable of utilizing both hexose and pentose sugars simultaneously. *Saccharomyces cerevisiae* (MTCC 181) was courteously provided by Institute of Microbial Technology (IM Tech), Chandigarh, India. The fermentation media was made from the hydrolysate derived from both the pre-treatment and enzymatic saccharification stage. The media was supplemented with the following: NH_4Cl 0.5 g/l; KH_2PO_4 2 g/l; $MgSO_4.7H_2O$ 0.5 g/l; yeast extract 1.5 g/l; $CaCl_2.2H_2O$ 0.1 g/l; $FeCl_3.2H_2O$; $ZnSO_4.7H_2O$ 0.001 g/l. The supplemented hydrolysate is autoclaved and then inoculated with 10% (v/v) of the seed cultures of *P. stipitis, C. shehatae* and *S. cerevisiae* at pH 5. The cultures are incubated at 30 °C at 150 rpm agitation speed for 36 hours. Samples were withdrawn and centrifuged at 10, 000 ×g at 4 °C. The supernatant was extracted and filtered using 0.45 μm PES membrane filters. Ethanol concentration was estimated by gas chromatography (GC) using flame ionisation detector (FID). The operating condition for GC were: detector temperature 250 °C, mobile phase: nitrogen (flow rate: 30 ml/min), column temperature: 150 °C, injector temperature: 175 °C and volume of injection: 1 μl. The samples were analysed three times and the mean value was presented.

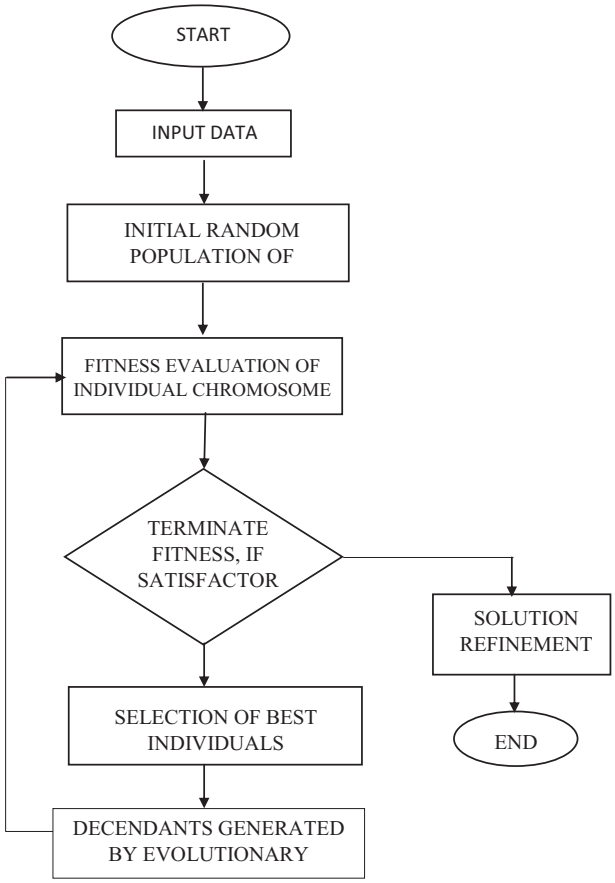

Fig. 1. The primary steps of a characteristic Genetic Algorithm model.

3. Results and discussion

3.1. Characterisation and compositional study of untreated and treated biomass

The cellulose, hemicellulose and total lignin content of the respective biomass are presented in Table 3. Alkali pre-treatment resulted in a 39.87% material loss, while on further enzymatic saccharification a total of 72.29 % material is lost. It was observed that after alkali pre-treatment the cellulose content almost remained untouched, but significant lignin content (86.76%) was lost. Hence, alkali pre-treatment was an effective delignification process. The alkali pre-treatment targets the cross linking ester bonds between the hemicellulose and lignin resulting in the saponification of the intermolecular bonds. Overall the alkaline pre-treatment induces increase in surface area, disordering

Table 1
Experimental range and levels of independent process variables.

Factor	Name	Low	High
A	Substrate concentration,(% w/w)	4	10
B	Cellulase loading, (U/g)	20	50
C	Xylanase loading, (U/g)	150	300
D	Surfactant concentration, (% w/w)	0.1	0.2

Table 2
Comparative result of observed and predicted results of xylose yield as a response using RSM and ANN model.

Run	Substrate concentration, (% w/w)	Cellulase concentration, (U/g)	Xylanase concentration, (U/g)	Surfactant concentration, (% w/w)	Total Reducing Sugar (TRS), (g/g)		
					Experimental	Predicted	
						ANN	RSM
1	7	35	150	0.1	0.457	0.456	0.456
2	7	50	225	0.2	0.511	0.51	0.5099
3	7	35	300	0.1	0.493	0.4931	0.4935
4	7	20	225	0.2	0.485	0.4861	0.4843
5	4	50	225	0.15	0.472	0.473	0.4713
6	7	20	225	0.1	0.458	0.4672	0.4935
7	10	20	225	0.15	0.487	0.864	0.4854
8	7	20	150	0.15	0.451	0.4523	0.4532
9	7	35	300	0.2	0.512	0.511	0.5101
10	7	35	150	0.2	0.464	0.463	0.4616
11	7	35	225	0.15	0.518	0.518	0.5184
12	10	35	150	0.15	0.482	0.4812	0.4805
13	10	35	225	0.2	0.517	0.5187	0.5225
14	7	35	225	0.15	0.513	0.5176	0.5184
15	4	35	300	0.15	0.468	0.4654	0.469
16	7	50	225	0.1	0.512	0.5127	0.5135
17	7	50	300	0.15	0.5353	0.5355	0.5357
18	7	50	150	0.15	0.428	0.4343	0.4308
19	7	20	300	0.15	0.434	0.4356	0.436
20	7	35	225	0.15	0.522	0.5178	0.5184
21	10	35	225	0.1	0.524	0.5344	0.5245
22	4	35	225	0.2	0.479	0.4844	0.4812
23	7	35	225	0.15	0.515	0.5245	0.5183
24	4	35	150	0.15	0.413	0.4135	0.4131
25	10	35	300	0.15	0.509	0.512	0.5097
26	4	20	225	0.15	0.433	0.433	0.4334
27	7	35	225	0.15	0.523	0.5224	0.5184
28	10	50	225	0.15	0.5297	0.5442	0.5273
29	4	35	225	0.1	0.462	0.4682	0.4577

the lignin structure, breaking structural intermolecular bonds between carbohydrates and lignin and finally separating lignin from the biomass matrix [19]. After enzymatic hydrolysis the cellulose content reduced by 68.34% and hemicellulose solubilisation increased to 90.45%.

To better support the observations in Table 3, SEM, XRD and FTIR based instrumental analysis were performed. SEM of WHB is shown in Fig. 2. The untreated WHB samples showed a firm, and highly ordered structure, while the treated samples exhibited dispersed and distorted structures. Enzyme hydrolysed WHB underwent greater degree of disruption than alkali pre-treated WHB. Similar observations were also reported for rice straw [19].

The FTIR spectra of the WHB are represented in Fig. 3, indicating changes in the shape, location and transmittance of the FTIR spectral bands. Band widening at 3400 cm^{-1} can be correlated to the stretching of the H-bonded hydroxyl (—OH) functional groups. Absorption peaks at 2940 cm^{-1} corresponds to –C-H stretching of the alkanes which is enhanced after alkali pre-treatment and enzymatic hydrolysis. The peak at 1735 cm^{-1} can be observed due to either acetyl or uronic ether linkages of carboxylic group in the ferulic and p-coumeric acids. Ferulic and p-coumeric acids are important components in lignin biopolymer. Disappearance of the 1735 cm^{-1} peak from the alkali pre-treated WHB sample indicates an effective de-lignification. The absorption peak at 1637 cm^{-1} can be attributed to the adsorbed water in the biomass sample. 1468 cm^{-1} represents the asymmetric bending of $–CH_3$. A characteristic band at 1398 cm^{-1} corresponds to the C = C linkages, which is present in the guaiacyl ring of the lignin. This absorption peak is present distinctly in the untreated sample. But there is significant reduction of this peak intensity for the alkali pre-treated and the enzyme hydrolysed sample implying lignin depolymerisation by pre-treatment. The band widening at 1318 cm^{-1} can be imputed to the CH_2 wagging vibrations present in the cellulose and hemi-cellulose. Similar observation is reported by Sun et al. for pre-treating bamboo biomass using formic acid [20]. The vibrational modes of the $–CH_2OH$ groups and the stretching of the IR spectra of the C-O bonds which are normally coupled with C-O bending of the C-OH functional groups of the carbohydrates can be responsible for the spectral bands at 1045 cm^{-1}. This spectral absorption normally indicates the decrease in the xylan content in the biomass by solubilisation of hemi-cellulose. Finally an absorption peak at 897 cm^{-1} explains a C-O-C stretching present in the β-(1, 4)-glycosidic linkage in cellulose and hemicellulose [21].

Table 3
Compositional analysis of untreated and treated WHB.

Components (% w/w)	Untreated WHB	Alkali pre-treated WHB	Enzyme hydrolysed WHB
Cellulose	34.6	31.027	10.981
Hemicellulose	29.3	17.71	8.814
Total Lignin	21.4	2.834	2.563
Others	14.7	8.56	5.346
Material loss	-	39.87	72.96

X-ray diffractograms of WHB are represented in Fig. 4. The untreated WHB sample has a CrI of 44.85%, while the alkali pre-treated and enzyme hydrolysed WHB samples have CrI 61.74% and 62.72% respectively. The hydrolysis of the glycosidic linkages helps in the removal of the amorphous hemi-cellulose and lignin, and renders the crystalline cellulose regions more accessible, resulting in the increase in the crystallinity index of the biomass. Similar results also have been reported [22]. The crystallinity index, crystallinity degree and crystalline size of WHB are

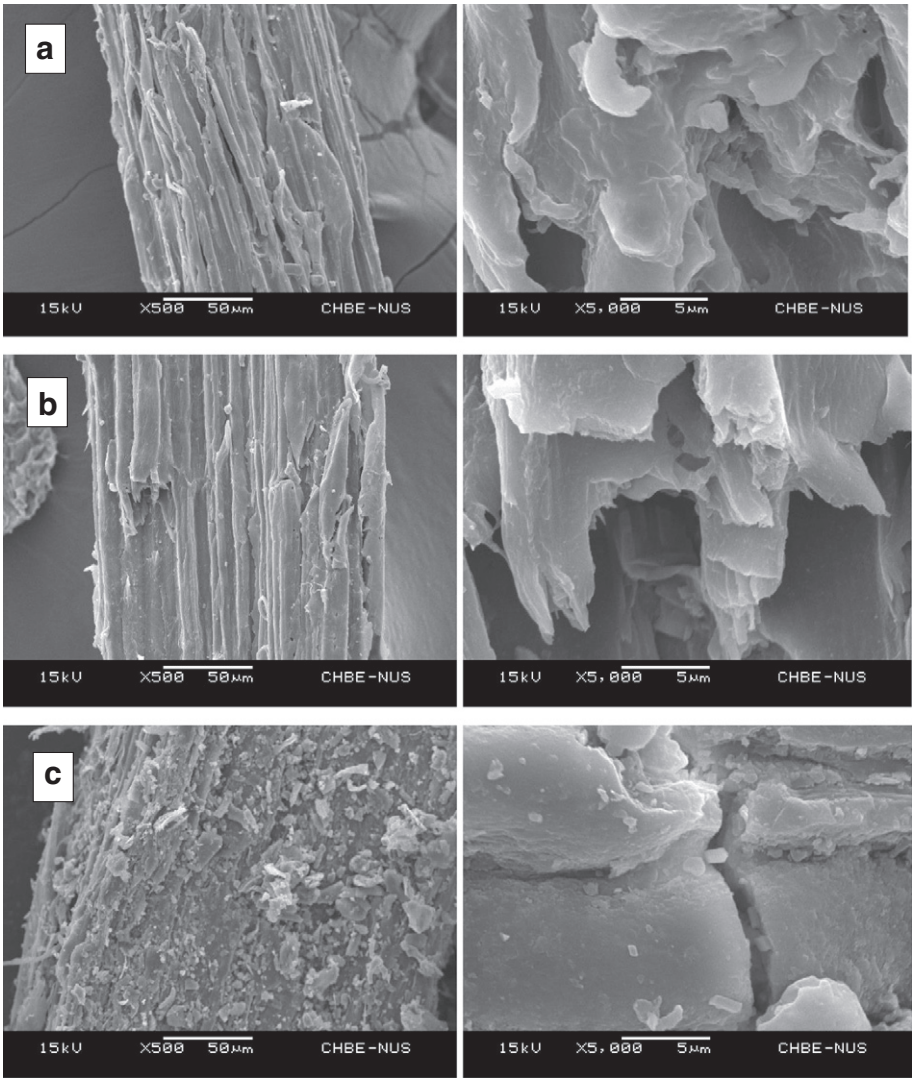

Fig. 2. Scanning electron micrographs of (a) untreated, (b) alkali treated and (c) enzyme hydrolysed WHB.

tabulated in Table 4. The crystalline size for the untreated sample is 0.203 nm, while for alkali pre-treated and enzyme hydrolysed samples 0.1741 nm and 0.152 nm respectively. The crystallinity degree (%) for untreated sample is 58.6%, which increased to 78.12% and 84.34% for alkali pre-treated and enzyme hydrolysed WHB respectively. Similar observations are reported for microwave pre-treated sugarcane bagasse [23].

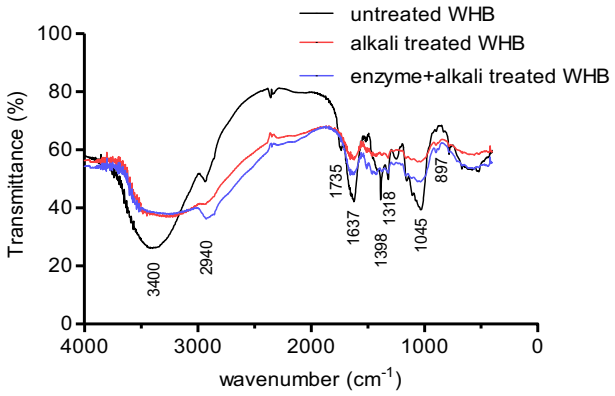

Fig. 3. FTIR spectra of untreated and treated water hyacinth biomass.

3.2. Theoretical maximum ethanol yield

Cellulose is homo-polysaccharide made of β-D-glucopyranose units, which are attached to each other by β-(1–4)-glycosidic linkages.

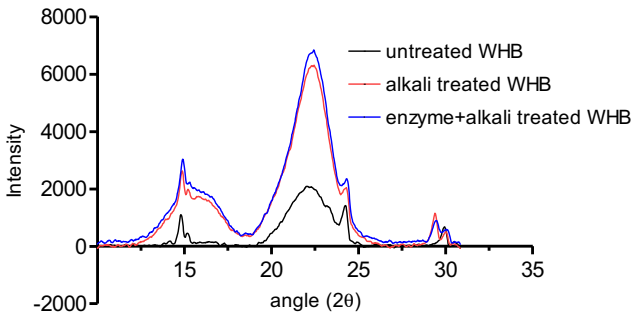

Fig. 4. X-ray diffraction pattern for untreated and treated WHB.

Table 4
Crystallinity index, crystalline size and crystallinity degree for WHB biomass.

Sample	Crystallinity index (%)	Crystalline Size (nm)	Crystalline degree (%)
WHB-untreated	44.85	0.203	58.6
WHB-alkali pre-treated	61.74	0.1741	78.12
WHB-enzyme hydrolysed	62.72	0.152	84.34

Cellulose can be hydrolysed by cellulase enzymes. These enzymes synergistically hydrolyse cellulose to cellobiose and glucose. On the other hand hemi-cellulose being structurally more complex than cellulose requires much more number of enzymes. The multi enzyme system for xylan hydrolysis includes endoxylanase, exoxylanase, β-xylosidase, α-arabinofuranosidase, α-glucoronisidase, acetyl xylan esterase, and ferulic acid esterase. The role of feruloyl esterases enzyme is to free hemi-cellulose from the linkages with lignin, to make the biomass more accessible for other enzymes.

Untreated WHB in this study contains 34.6% (w/w) of cellulose and 29.3% (w/w) of hemi-cellulose. Assuming that the cellulose in the biomass is fully converted to glucose $\left[(C_6H_8O_4)_n + nH_2O \rightarrow nC_6H_{12}O_6 : 34.6\% \times \frac{180}{(180-18)} = 38.44\%\right]$ followed by a full conversion of hemi-cellulose to xylose $\left[(C_5H_8O_4)_n + nH_2O \rightarrow nC_5H_{10}O_5 : 29.3\% \times \frac{150}{(150-18)} = 33.295\%\right]$, a maximum theoretical reducing sugar yield of 0.7174 g per 1 g of untreated water hyacinth biomass. Theoretically we can obtain 0.51 kg of ethanol per kilogram of glucose and xylose. Hence, the maximum theoretical ethanol yield possible is 0.3659 g/g of WHB.

3.3. ANN-GA hybrid modelling and optimisation

Table 2 have been used to construct and train the neural network. Overall, N = 29 data points are used to construct the neural network model. 80% of the total experimental data is used for training the network while the rest is kept for testing and validation of the model. The inputs and the targets are normalised before the training exercise. The purpose of normalising is to avoid overflow situations. The Neural Network Toolbox V4.0 in MATLAB is used for building the artificial neural network model.

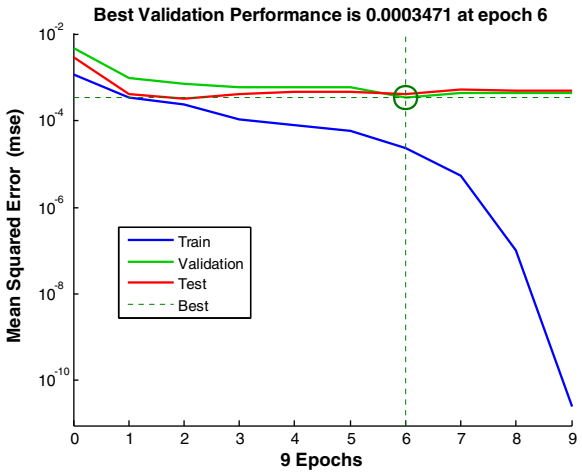

Fig. 6. Development of MSE during training phase of ANN model.

The optimal structure of the feed-forward network model for the neural network is represented in Fig. 5. The weights of the input layer are represented by an input weight matrix $\mathbf{IW^{(1,1)}}$. The weight matrix of the layer is represented by $LW^{(2,1)}$. The source and the destination connections are denoted by the superscripts. The bias in each layer is indicated by $\mathbf{b^{(1)}}$. Here the superscript implies the layer. This neural network is trained using Levenberg-Marquardt back propagation method to determine the values of weights and biases. Training of the neural network is enforced to stop when the error of the network (MSE) drops significantly to a low value (MSE $\leq E_o$, where the goal E_o is set at 5×10^{-4}). In the present study, the training terminated after 9 iterations (epochs). Fig. 6 indicates the development of the MSE of the neural network during the training phase. The final point of the training data has a performance function MSE lower than the set goal (Fig. 6), indicating a successful end of network training and hence the optimised results for the weights and biases (Table 5). The performance plot (Fig. 6) implies (i) small final mean square error; (ii) test set error and the validation mean square error have similar characteristics and (iii) no overfitting.

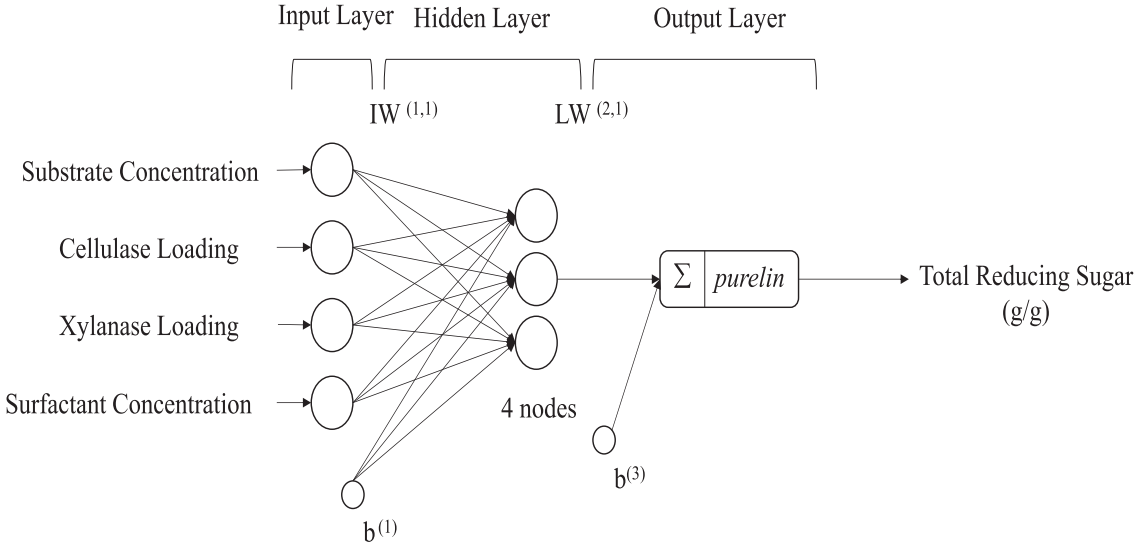

Fig. 5. Topology of the neural network model used to predict enzymatic saccharification of WHB.

Table 5
Optimal values of weights and biases obtained by training ANN model.

Weights to Hidden layer from Inputs	$\mathbf{IW}^{(1,1)} = \begin{vmatrix} -1.3921 & -1.1228 & -0.53079 & 0.99857 \\ 0.9707 & 0.6113 & 0.8316 & 0.71181 \\ -0.8393 & 0.9223 & 0.8387 & -1.2267 \\ -1.1452 & 0.5082 & 0.8661 & 1.2429 \end{vmatrix}$
Bias vector to hidden layer	$\mathbf{b}^{(1)} = \lvert 0.18522 \quad -0.01407 \quad -1.1064 \quad -2.0499 \rvert^{T}$
Weights to output layer from hidden layer	$\mathbf{LW}^{(2,1)} = \lvert 0.5271 \quad 0.63418 \quad 0.091 \quad 0.0898 \rvert$
Bias vector to output layer	$\mathbf{b}^{(2)} = \lvert 0.8128 \rvert^{T}$

The statistical significance of the developed model was tested by analysis of variance (ANOVA) and is represented in Table 6. ANOVA for the neural network model has a *F-value* of 234.54 with *p-value* 0.0021 implying the model is significant. The closeness between experimental and predicted values by the model is represented in Fig. 7. A very high value of correlation co-efficient ($r^2 = 0.9996$) and adjusted co-efficient (adj.$R^2 = 0.9982$) illustrate that the developed ANN model is significant and can used to predict the optimal topology.

The quality of the data used for developing the ANN model is estimated by the error histogram plot. We can observe that most of the errors lies in between −0.003 and 0.003 (Fig. 8), but there are validation data points with error as high as 0.0169 as compared to the rest of the data set. Outliers are used to determine the quality of the given data. Large number of outliers in this model necessitated collection of more data points to improve the network.

Overall the generalisation potentiality of the developed neural network model has been improved by applying the following techniques: (i) normalisation, (ii) optimal number of neurons and (iii) dividing the target data into training, validation and test data subsets.

Genetic Algorithm was implemented to optimise the ANN model. The evolution of the profile to search the optimum condition by GA is represented in Fig. 9. It took 51 generations for GA to converge to the optimal point, with the optimal condition of the saccharification of the alkali pre-treated WHB: substrate concentration 9.012 % (w/w), cellulase loading 49.997 U/g, xylanase loading 282.04 U/g and surfactant concentration of 0.122 % (w/w). The maximum total reducing sugar obtained at this optimal condition is 0.5672 g/g theoretically. The accuracy of the optimised condition was verified by validation experiments. Experimentally, a total reducing sugar concentration of 0.5618 g/g at the optimum condition was obtained, thus showing that the optimum condition predicted by the ANN-GA hybrid technique was precise.

3.4. Response surface methodology

The interaction of the independent factors affecting the enzymatic saccharification of WHB was determined by Box-Behnken full factorial design. Table 7 summarises the results obtained for the ANOVA study. The statistical significance of the model is determined by F-test ANOVA. A p-value less than 0.05 imply the significance of the corresponding variable [24]. The independent parameters viz. substrate concentration, cellulase loading, xylanase loading and surfactant concentration have a significant influence on the yield of total reducing sugar during enzymatic hydrolysis (Table 7). The non-significant value of lack of fit and a significant value for model proved the validity of the quadratic model. This model for RSM proved to be highly significant due to its high Fisher's F-value (241.1) with a low probability value ($p < 0.0001$). Regression co-efficient (r^2) came out to be 0.9959. The predicted R-squared (0.9844) and the adjusted R-squared (0.9917) are in reasonable argument with each other. The residual variation is measured using co-efficient of variance (CV) relative to the size of the mean. A very low (0.64%) value of CV implies a sufficient precision and reliability on the experimental results. Predicted Residual Sum of Squares (PRESS) is another parameter to express the fitness of the model. The smaller the PRESS statistic, the better the model fits the data points. In the present study the calculated value of PRESS is 5.2. The standard deviation and mean values came as 0.037 and 0.49

Table 6
ANOVA for neural network model.

Source	DF	SS	MS	F-value	P-value	R^2	Adj. R^2
Model	24	0.034	0.0023	234.54	<0.0001	0.9996	0.9982
Residual	4	0.00014	0.000009				
Total	28	0.03414					

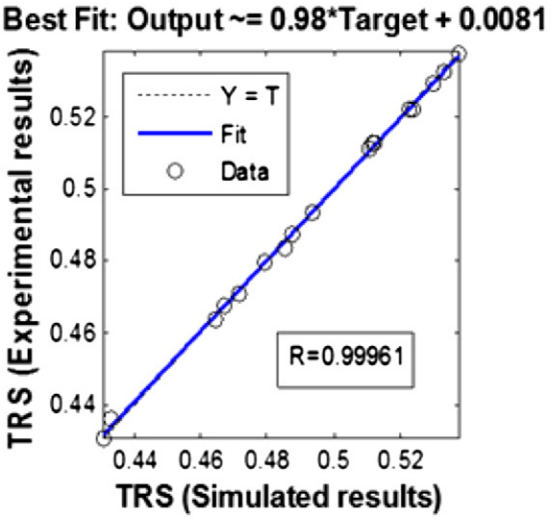

Fig. 7. The plot of experimental data vs ANN model predicted data.

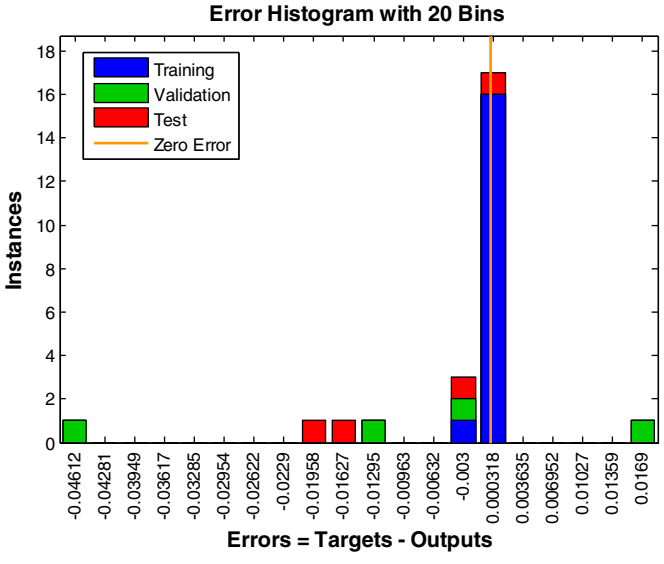

Fig. 8. Error histogram plot for the ANN model for enzymatic saccharification of WHB.

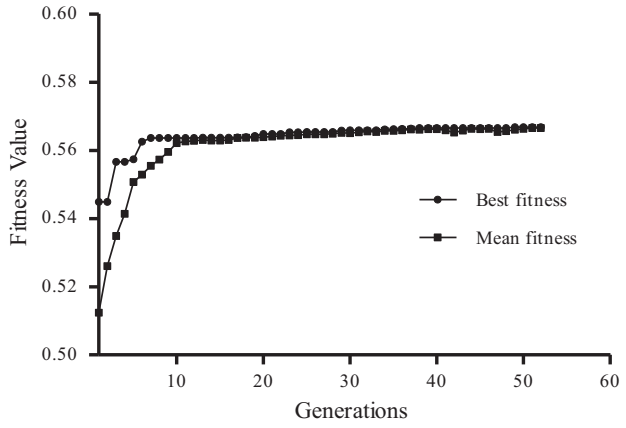

Fig. 9. Evolution of the fitness value over a generation of 51 generation.

respectively. The corresponding second order model obtained after ANOVA study:

$$\begin{aligned}\text{Total reducing sugar (TRS)} = {} & -0.116 + 0.048 * \text{substrate concentration} \\ & + 0.0032 * \text{cellulase loading} \\ & + 0.0021 * \text{xylanase loading} \\ & + 1.13 * \text{surfactant concentration} \\ & + 0.00002 * \text{substrate concentration} \\ & * \text{cellulase loading} \\ & - 0.00003 * \text{substrate concentration} \\ & * \text{xylanase loading} \\ & - 0.042 * \text{substrate concentration} \\ & * \text{surfactant concentration} \\ & - 00003 * \text{cellulase loading} * \text{xylanase-0.095} \\ & * \text{cellulase loading} * \text{surfactant concentration} \\ & + 0.0008 * \text{xylanase loading} \\ & * \text{surfactant concentration} - 0.002 \\ & * \text{substrate concentration}^2 \\ & - 0.0001 * \text{cellulase loading}^2 \\ & - 0.00001 * \text{xylanase loading}^2 \\ & - 1.189 * \text{surfactant concentration}^2\end{aligned}$$

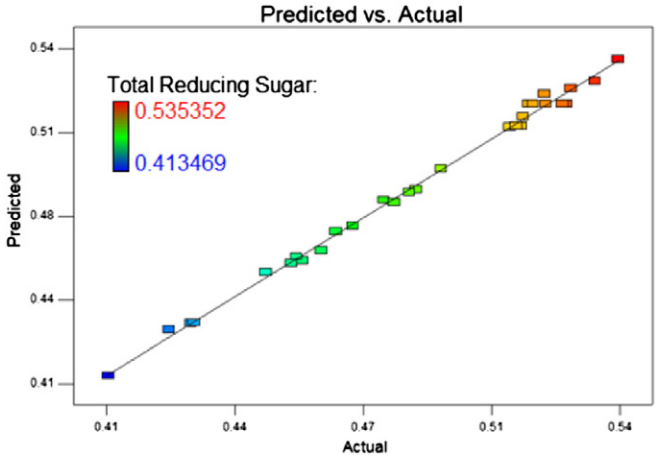

Fig. 10. Experimental data plotted against RSM model predicted data for enzymatic hydrolysis of WHB.

The goodness of fit of the RSM model is represented in Fig. 10. Most of the experimental results lie on the 45 degree line implying that the model predicted results are very close in agreement with the experimental data.

The interaction effect of the process parameters on the total yield of reducing sugar for enzymatic saccharification of WHB are studied using the three dimensional plots (Fig. 11a–f).

Fig. 11a represents total reducing sugar yield as a function of substrate concentration and cellulase loading. At low level of substrate concentration and cellulase loading, a very low yield of reducing sugar was observed. The yield of reducing sugar has increased with the increase in cellulase loading and substrate concentration. A slight dip in the yield of reducing sugar is observed at the highest levels. This may be caused due to feedback inhibition of the system.

Fig. 11b presents the yield of reducing sugar as a function of xylanase loading and substrate concentration. It is observed from the figure, the yield of reducing sugar increases as one move from the lower levels of the factors to the middle levels and then there is a reduction in the yield. This can be explained due the presence of the inhibitory factors which can cause a feedback repressive effect.

Table 7
Analysis of variance of quadratic RSM model.

Source	SS	d*f*	Co-efficient	*F*-value	*p*-value Prob > F
Model	0.033	14	0.52	241.1	<0.0001 (Significant)
A – Substrate Concentration	0.0088	1	0.027	888.91	<0.0001
B – Cellulase loading	0.0048	1	0.02	485.07	<0.0001
C – Xylanase loading	0.0054	1	0.021	553.44	<0.0001
D – Surfactant Concentration	0.00035	1	0.00536	35.07	<0.0001
AB	0.000004	1	0.001	0.41	0.0531
AC	0.00018	1	−0.0067	18.23	<0.0001
AD	0.00016	1	−0.0064	16.67	<0.0001
BC	0.0039	1	0.031	393,93	<0.0001
BD	0.0002	1	−0.00713	20.84	<0.0001
CD	0.00009	1	0.00296	3.56	0.0018
A^2	0.00191	1	−0.017	19.24	<0.0001
B^2	0.00311	1	0.0022	315.42	<0.0001
C^2	0.00713	1	−0.022	724.32	<0.0001
D^2	0.00015	1	−0.033	14.81	0.0018
Residual	0.00014	14			
Lack of Fit	0.000073	10		0.45	0.8643 (Non-Significant)
Pure Error	0.000063	4			
Model statistics					
Std. Dev.	0.317	R-squared	0.9959		
Mean	0.49	Adj. R-squared	0.9917		
C.V. %	0.64	Pred. R-squared	0.9844		

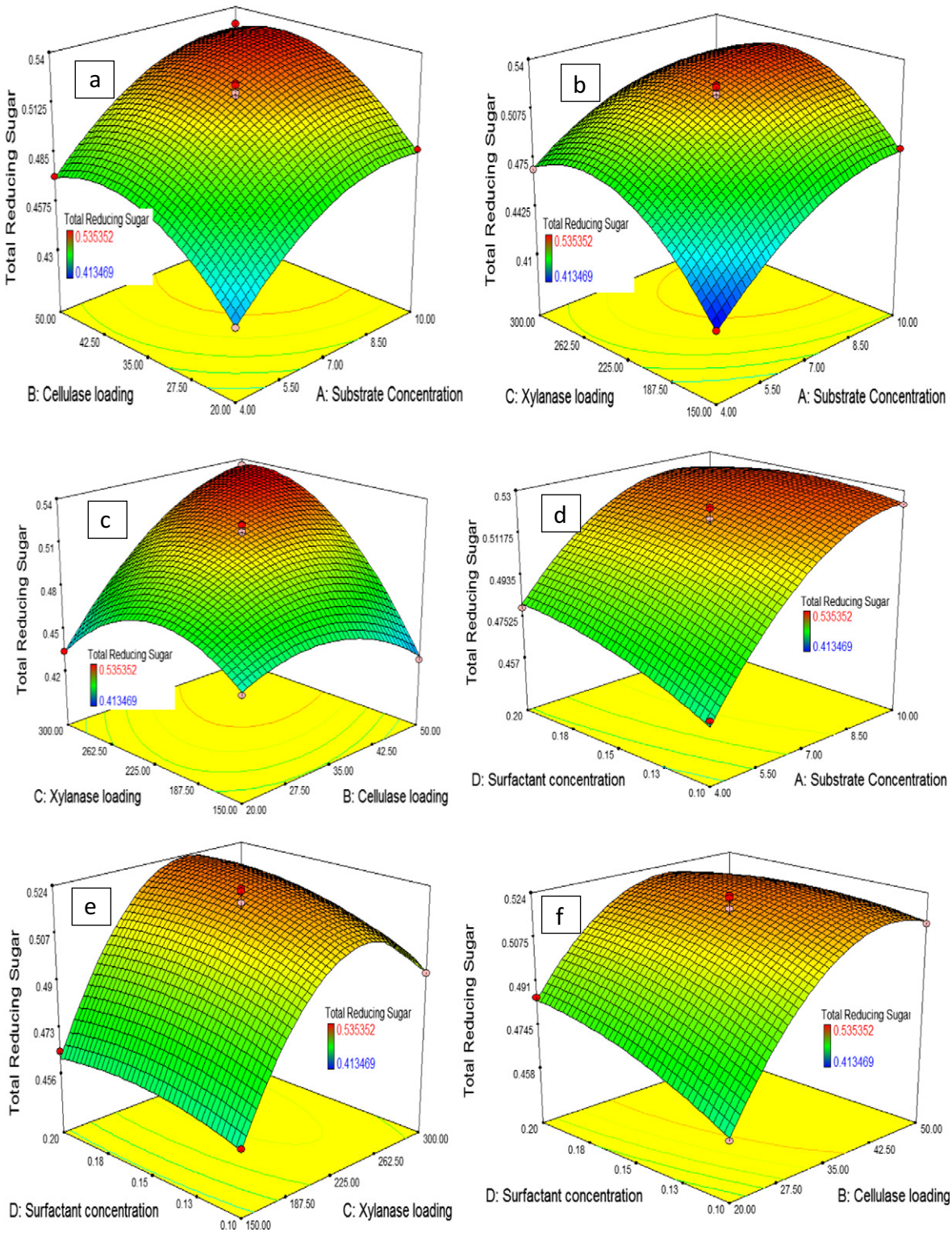

Fig. 11. Effect of operating parameters on the enzymatic saccharification of alkali pre-treated WHB for reducing sugar yield (a) Effect of substrate concentration and cellulase loading on reducing sugar yield. (b) Effect of substrate concentration and xylanase loading on reducing sugar yield. (c) Effect of xylanase loading and cellulase loading on reducing sugar yield. (d) Effect of substrate concentration and surfactant concentration on reducing sugar yield. (e) Effect of surfactant concentration and xylanase loading on reducing sugar yield. (f) Effect of surfactant concentration and cellulase loading on reducing sugar yield.

The effect of cellulase and xylanase loading is explained by the Fig. 11c. At low levels of cellulase and xylanase loading a very low yield of reducing sugar is observed, because of low concentration of enzymes. As the concentration of cellulase and xylanase increased there is a significant increase in the yield, indicating a synergistic effect of the enzymes on the saccharification process. At the highest level of the factor, however, a slight reduction in the yield of the total reducing sugars is noticed. At high loading of enzymes, the function of the individual

Table 8
Comparison of predictive potentiality between RSM and ANN model.

Statistical parameters	Design data		Validation data	
	ANN	RSM	RSM	ANN
Correlation coefficient	0.9993	0.9959	0.9985	0.9878
Percentage avg. error	3.08	4.82	3.4	5.2
RSME	0.24	0.32	0.54	0.78

enzymes may get curbed due to a change in the surface properties of the enzymes at such high concentration, resulting in the decrease of productivity of total reducing sugar [25].

The effect of surfactant concentration and substrate concentration on the yield of reducing sugar by enzymatic saccharification is represented in Fig. 11d. At initial level of both the factors, a very low yield from the enzymatic hydrolysis is observed. Maximum reducing sugar yield is obtained at the highest level of surfactant concentration (0.2% w/w) and substrate loading (10% w/w). The function of surfactant is to modify the surface properties of the substrate, so as to increase the availability of cellulose and hemi-cellulose for the enzymes. The surfactants also help in removing the remaining inhibitory lignin and hence a synergistic effect of the two parameters for increasing the reducing sugar yield is noticed [25].

Fig. 11e explains the yield of total reducing sugar as a function of surfactant concentration and xylanase loading. It is very much evident from the figure that at low levels of both the parameters there is low yield of the response. But the reducing sugar concentration increased eventually with the increase in xylanase loading up to 275 U/g, after which a significant dip in the yield is observed. Hence according to this figure, it can be inferred that high level of surfactant concentration (0.2% w/w) and middle level of xylanase loading result in the highest yield of reducing sugar. Addition of surfactants normally prevents the unfruitful addition of enzymes to lignin region by modifying the surface properties of the biomass. Overall surfactant addition has a positive impact on the saccharification process. However at high levels of xylanase concentration the yield might have decreased due to the feedback inhibition effect or over modification of surface properties of the biomass leading to reduction in the functional property of the enzyme.

The interaction between the cellulase loading and surfactant concentration is represented in Fig. 11f. The overall trend of the surface plot is very similar to Fig. 11e. Here a low yield of reducing sugar at low levels of cellulase and cellulase loading is seen. Highest yield of reducing sugar is obtained at high level of surfactant concentration (0.2% w/w) and middle level of cellulase concentration. Similar trend was reported; a 63 % increase in saccharification efficiency for steam pre-treated spruce wood occurred when supplemented with Tween-20 [26]. In this current study Tween-80 have been incorporated and a positive impact of the surfactant on the saccharification efficiency was found.

To optimise the process parameters in the RSM approach, a desirability function was implemented. The best optimum for the response is predicted at a substrate concentration of 9.92 % (w/w), cellulase loading of 49.56 U/g, xylanase loading of 280.33 U/g and surfactant concentration of 0.13 % (w/w). At this optimum condition the maximum total reducing yield predicted by the model is 0.5447 g/g. The predicted optimum condition was validated experimentally where a yield of 0.5524 g/g of total reducing sugar was obtained.

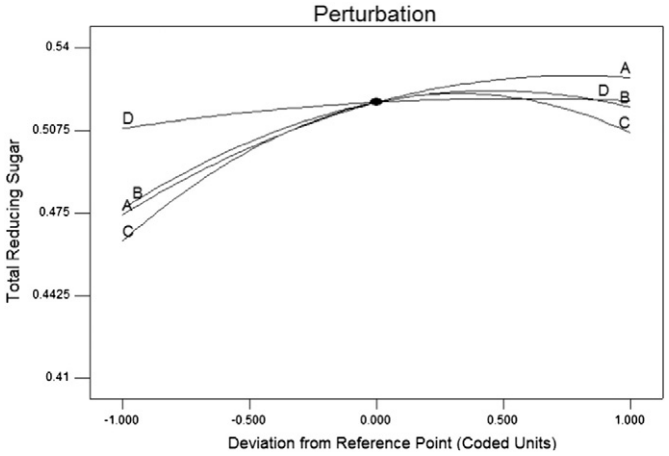

Fig. 12. Sensitivity analysis by perturbation method for ANN model.

3.5. Comparison between the hybrid ANN-GA model and RSM

3.5.1. Prediction potentiality

The effectiveness of the models were tested by examining statistical parameters such as the average % error, RMSE and correlation coefficient (CC). The calculated values of average % error, CC and RSME, presented in Table 8, proves that the MLP-based artificial neural network model fitted the experimental result better compared to RSM.

To judge the effectiveness of both the models, we tested the model with a total new set of unseen dataset. The experimental and predicted values of reducing sugar yields are tabulated in Table 9. The CC for the unseen data set for ANN and RSM models are 0.9985 and 0.9878 while for average error percentage are 3.4 and 5.2 respectively. It is evident that ANN has a better potential for generalisation compared to RSM model. The reason for this better performance can be accredited to its ability to approximate diverse set of non-linear polynomials, whereas RSM is only capable of capturing only quadratic approximations.

3.5.2. Sensitivity analysis

The calculated co-efficients in RSM model provide a straight forward measure of the degree of contribution of each of the factors. Biomass loading has the largest co-efficient (0.027), implying that substrate concentration is the most significant factor in the model. Next in importance is the enzyme loading: cellulase and xylanase concentration. An examination of the interaction effects amongst the factors show that synergistic effect between the two enzymes is the most significant in the system.

Table 9
Validation data set for the RSM and ANN model.

Run	Substrate concentration, (% w/w)	Cellulase concentration, (U/g)	Xylanase concentration, (U/g)	Surfactant concentration, (% w/w)	Total Reducing Sugar (TRS), (g/g)		
					Experimental	Predicted	
						ANN	RSM
1	2	10	100	0.05	0.0589	0.595	0.611
2	15	75	350	0.25	0.411	0.409	0.397
3	10	75	225	0.2	0.423	0.4215	0.417
4	10	75	300	0.15	0.5145	0.5153	0.5176
5	10	50	350	0.1	0.5182	0.5246	0.523

Table 10
Optimum condition for enzymatic hydrolysis of alkali pre-treated WHB for maximum TRS using different techniques.

Optimisation Strategies	Substrate concentration, (% w/w)	Cellulase concentration, (U/g)	Xylanase concentration, (U/g)	Surfactant concentration, (% w/w)	Total Reducing Sugar (TRS), (g/g)	
					Experimental	Predicted
Centre point of DOE	7	35	225	0.15	0.518	-
ANN-GA hybrid	9.92	49.56	280.33	0.13	0.5618	0.5672
RSM	9.012	49.99	282.04	0.122	0.5524	0.5547

Numerical methods are required to capture the intrinsic nature of the ANN model. Perturbation method (Fig. 12) is one such approach used to examine the sensitivity analysis of the ANN model. The influence of a variable can be estimated based on the slope and range of change; the greater the slope and the range, the higher is the expected influence of that independent variable on the system. The substrate concentration has the highest slope and hence can be considered as the most significant factor which influences the enzymatic saccharification process. This observation is similar to that of RSM. Thus ANN can also be used as an effective model for sensitivity analysis.

3.5.3. Optimisation results

Table 10 tabulates the summary of optimised parametric condition for enzymatic saccharification using different approaches. The optimum condition predicted by ANN-GA hybrid and RSM are almost similar except for the substrate concentration and xylanase loading. ANN-GA hybrid model predicted the total yield of reducing sugar to be 0.5672 g/g at the optimum level of process parameters. Experimentally validation gave a yield of 0.5618 g/g. Similarly, the experimental and predicted responses for the RSM model for the enzyme saccharification process at the optimal condition are 0.5524 g/g and 0.5447 g/g respectively. The prediction error in optimal yield for the enzymatic hydrolysis process by the ANN-GA hybrid model is 0.95% while for RSM model it was 1.41%. It was observed that the prediction error for RSM model was quite large compared to the ANN-GA hybrid. Hence even with not much of a difference between the predictive yields by both the model, ANN-GA hybrid model has more precision in predicting the optimum condition.

3.6. Fermentation

Fermentation experiments were performed in shake flasks using *Candida shehatae, Saccharomyces cerevisiae* and *Pichia stipitis*. A highest ethanol yield of 10.44 g/l (equivalent to 0.1044 g/g) was obtained with *Pichia stipitis*, followed by 8.24 g/l (0.0824 g/g of WHB) with *Candida shehatae* and 6.76 g/l (0.0676 g/g of WHB) with *S. cerevisiae*. *P Stipitis* can utilise both pentose and hexose sugar to produce ethanol. As the hydrolysate in the study contained both hexose and pentose sugars obtained from the hydrolysis of cellulose and hemi-cellulose, *P. stipitis* was able to produce a higher amount of ethanol than the other microorganisms. Still we are not able to achieve 50 % of the theoretical ethanol yield (Fig. 13). This dismal insignificant yield of ethanol can result due to the presence of inhibitory products which may be present in the hydrolysate. There are numerous reports which reveal that the presence of furfural or hydroxyl methyl furfurals causing intense inhibitory effect on ethanol production. These substances act by inhibiting the central enzymes responsible for ethanol production in the yeasts like hexokinase, phosphofructokinase and trios-phosphate dehydrogenase [27]. Hence if the hydrolysate is detoxified, a higher ethanol yield may be expected.

4. Conclusion

The primary focus was on enhancing fermentable sugars from WHB by enzymatic saccharification process. The WHB was first pre-treated under alkaline condition to remove almost 86.76% of lignin. Following this, the process parameters for enzymatic saccharification was optimised using Box Benhken and ANN-GA hybrid model. The physical changes in the characteristics of the treated biomass were well captured by different instrumental analysis viz. SEM, XRD, FT-IR. The process parameters selected for the enzymatic hydrolysis were optimised. Comparison between the optimisation models were made based on predictive potentiality, sensitivity analysis, and optimisation efficiency for enzymatic saccharification. ANN proved to have a higher accuracy in modelling than RSM. Thus, it is concluded that alkali pre-treatment is an effective method to remove lignin and improve enzymatic saccharification and ANN-GA hybrid model may present a better alternative to the most widely used RSM technique for optimising saccharification process.

Acknowledgements

The authors are grateful to Director, CSIR-Central Mechanical Engineering Research Institute, Durgapur, India for constant support, encouragement and permission to publish this paper.

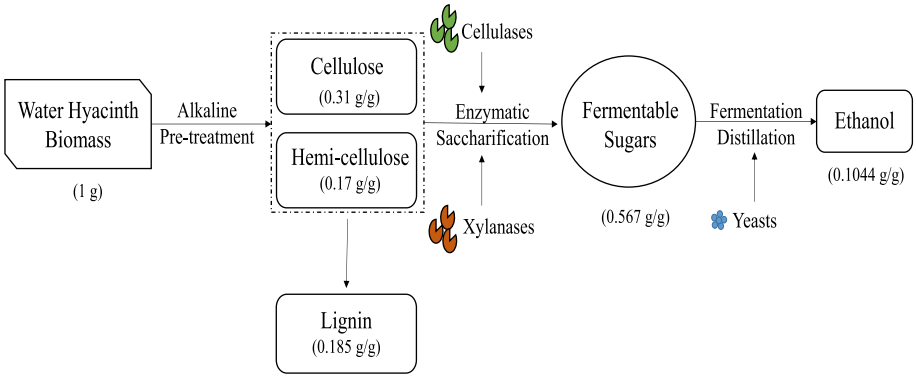

Fig. 13. Process flow diagram of the entire set of experiment.

References

[1] O. Merino-Pérez, R. Martínez-Palou, J. Labidi, R. Luque, Microwave-assisted Pretreatment of lignocellulosic biomass to produce biofuels and value-added products, Production of biofuels and chemicals with microwave, Springer, Netherlands, 2015. 197–224.

[2] A. Ganguly, S. Das, A. Bhattacharya, A. Dey, P.K. Chatterjee, Enzymatic hydrolysis of water hyacinth biomass for the production of ethanol: Optimization of driving parameters, Indian J. Exp. Biol. 51 (2013) 556–566.

[3] F. Rosillo-Calle, D. Hall, Brazilian alcohol: food versus fuel? Biomass 12 (1987) 97–128.

[4] M. Fatih Demirbas, Biorefineries for biofuel upgrading: a critical review, Appl. Energy 86 (2009) S151–S161.

[5] T. Mehmood, S.A. Malik, S.T. Hussain, Role of microbes in nitrogen and metal hyperaccumulation by taxilaion Eichhornia crassipes, Afr. J. Microbiol. Res. 3 (2009) 914–924.

[6] J. Nigam, Bioconversion of water-hyacinth (Eichhornia crassipes) hemicellulose acid hydrolysate to motor fuel ethanol by xylose–fermenting yeast, J. Biotechnol. 97 (2002) 107–116.

[7] A. Ganguly, A. Gupta, S. Das, A. Dey, P. Chatterjee, Enzymatic hydrolysis of water hyacinth substrate by cellulase, xylanase and glucosidase: Experiments and optimization, J. Biobased Mater. Bioenergy 6 (2012) 283–291.

[8] M. Tanaka, Effect of chemical treatment on solubilization of crystalline cellulose and cellulosic wastes with Pellicularia filamentosa cellulase, J. Ferment. Technol. 57 (1979) 186–190.

[9] A. Sluiter, B. Hames, R. Ruiz, C. Scarlata, J. Sluiter, D. Templeton, D. Crocker, Determination of structural carbohydrates and lignin in biomass, Laboratory analytical procedure2008.

[10] S. Das, A. Ganguly, A. Dey, Y.-P. Ting, P.K. Chatterjee, Characterization of water hyacinth biomass and microbial degradation of the biomass under solid state fermentation using a lignocellulolytic fungus (*Alterneria* Spp NITDS1), J. Chem. Biol. Phys. Sci. 4 (2014) 2279–2293.

[11] S.Y. Oh, D.I. Yoo, Y. Shin, G. Seo, FTIR analysis of cellulose treated with sodium hydroxide and carbon dioxide, Carbohydr. Res. 340 (2005) 417–428.

[12] G. MILLER, Use of dinitrosalicylic acid reagent for determination reducing sugar, Anal. Chem. 31 (1959) 426–428.

[13] B. Sarkar, A. Sengupta, S. De, S. DasGupta, Prediction of permeate flux during electric field enhanced cross-flow ultrafiltration – a neural network approach, Sep. Purif. Technol. 65 (2009) 260–268.

[14] M.T. Hagan, H.B. Demuth, M.H. Beale, Neural network design, Pws, Boston, 1996.

[15] D.E. Rumelhart, G.E. Hinton, R.J. Williams, Learning representations by back-propagating errors, Nature 323 (1986) 533–536.

[16] S.H.R. Pasandideh, S.T.A. Niaki, Multi-response simulation optimization using genetic algorithm within desirability function framework, Appl. Math. Comput. 175 (2006) 366–382.

[17] G. Renner, A. Ekárt, Genetic algorithms in computer aided design, Comput. Aided Des. 35 (2003) 709–726.

[18] K.J. Rao, C.-H. Kim, S.-K. Rhee, Statistical optimization of medium for the production of recombinant hirudin from Saccharomyces cerevisiae using response surface methodology, Process Biochem. 35 (2000) 639–647.

[19] J.K. Ko, J.S. Bak, M.W. Jung, H.J. Lee, I.G. Choi, T.H. Kim, K.H. Kim, Ethanol production from rice straw using optimized aqueous-ammonia soaking pretreatment and simultaneous saccharification and fermentation processes, Bioresour. Technol. 100 (2009) 4374–4380.

[20] Y. Sun, L. Lin, H. Deng, J. Li, B. He, R. Sun, P. Ouyang, Structural changes of bamboo cellulose in formic acid, BioResources 3 (2008) 297–315.

[21] M.L. Nelson, R.T. O'Connor, Relation of certain infrared bands to cellulose crystallinity and crystal lattice type. Part II. A new infrared ratio for estimation of crystallinity in celluloses I and II, J. Appl. Polym. Sci. 8 (1964) 1325–1341.

[22] A.O. Converse, R. Matsuno, M. Tanaka, M. Taniguchi, A model of enzyme adsorption and hydrolysis of microcrystalline cellulose with slow deactivation of the adsorbed enzyme, Biotechnol. Bioeng. 32 (1988) 38–45.

[23] P. Binod, K. Satyanagalakshmi, R. Sindhu, K.U. Janu, R.K. Sukumaran, A. Pandey, Short duration microwave assisted pretreatment enhances the enzymatic saccharification and fermentable sugar yield from sugarcane bagasse, Renew. Energy 37 (2012) 109–116.

[24] Ž.R. Lazić, Design and analysis of experiments: Section 2.3, Wiley Online Library, 2004.

[25] S.S. Helle, S.J. Duff, D.G. Cooper, Effect of surfactants on cellulose hydrolysis, Biotechnol. Bioeng. 42 (1993) 611–617.

[26] T. Eriksson, J. Börjesson, F. Tjerneld, Mechanism of surfactant effect in enzymatic hydrolysis of lignocellulose, Enzym. Microb. Technol. 31 (2002) 353–364.

[27] E. Palmqvist, B. Hahn-Hägerdal, M. Galbe, G. Zacchi, The effect of water-soluble inhibitors from steam-pretreated willow on enzymatic hydrolysis and ethanol fermentation, Enzym. Microb. Technol. 19 (1996) 470–476.